Sakarya University Journal of Science

ISSN : 2147-835X
Publisher : Sakarya University

Vol. 28, No. 5, 1070-1085, 2024
DOI: https://doi.org/10.16984/saufenbilder.1533467

Research Article

Experimental and Theoretical Characterization, In Silico and In Vitro Studies of (E)-1-(5-Nitrothiophen-2-yl)-N-(2-(Trifluoromethyl)Phenyl)Methanimine

Seyhan Öztürk

Ondokuz Mayıs University, Faculty of Science, Department of Chemistry, Samsun, Türkiye, sturna@omu.edu.tr

ARTICLE INFO

Keywords:
Schiff base
Crystal structure
Molecular docking
Hirshfeld surface analysis
Density Functional Theory

Article History:
Received: 14.08.204
Accepted: 01.09.2024
Online Available: 18.10.2024

ABSTRACT

The current research was conducted to assess the in silico and in vitro potential of the heterocyclic Schiff base compound (E)-1-(5-nitrothiophen-2-yl)-N-(2-(trifluoromethyl)phenyl)methanimine(N2TPM). This Schiff base was synthesized according to the reported method using ethanol as solvent, and the reaction was monitored on TLC till completion of the reaction. The compound structure was elucidated using spectroscopic techniques such as UV/Vis, FT-IR, ^{1}H-NMR, and ^{13}C-NMR. Molecular structure was determined using a single XRD, which revealed that the compound was triclinic. Analysis of intermolecular interactions in crystalline compounds was performed using Hirshfeld surface analysis and 2D fingerprint plots. The structure of the compound was optimized using the B3LYP hybrid functional with the basis set 6-31G(d,p). The compound's theoretical and experimental parameters (bond length, bond angle, molecular orbital energies, electronic transitions, and vibration frequencies) were compared with each other which are in close agreement. R^2 values were found to be 0.9914 for bond lengths and 0.9859 for bond angles. In vitro, esterase potential of the synthesized compound was checked using a spectrophotometric model, while in silico molecular docking studies were performed with Auto-dock against two enzymes of the esterase family. The docking studies and in vitro assessment predicted that such molecules could be used as enzyme inhibitors against tested enzymes; acetylcholine esterase (AChE) and butyrylcholine esterase (BChE). the compound showed a binding score of -10.4159, a binding energy of -10.2743 with AChE, a binding score of -10.3378 and a binding energy of -9.8889 with BChE.

1. Introduction

Schiff bases are synthesized by reacting aldehydes/ketones and amines in a suitable medium. These compounds have exhibited numerous valuable pharmacological applications, such as the inhibition of acetylcholine and butyrylcholine esterase enzymes, which are responsible for Alzheimer's disease [1–3]. Schiff bases also behave as ligands, coordinating with metals through imine nitrogen [4]. They possess exceptional properties, including stability, selectivity, and sensitivity. Researchers are continually creating different Schiff bases with varied structural attributes for significant applications [5, 6]. Schiff bases find broad application across various fields, biochemistry, separation processes, decarboxylation reactions, including catalysis, materials science, and enzymatic aldolization [7, 8].

Heterocyclic cores represent a major class of organic compounds characterized by the presence of at least one non-carbon atom (heteroatom) within the ring structure. These compounds acquire different properties due to their compressed structure, such as anti-corrosion, anti-oxidant, and anti-wear properties. Heterocyclic compounds play a fundamental role in the cells of living organisms, exhibiting vast dimensional applications in different fields, including veterinary products, pharmaceuticals, and agrochemicals [9, 10]. These compounds are

Cite as: S. Öztürk (2024). Experimental and Theoretical Characterization, In Silico and In Vitro Studies of (E)-1-(5-Nitrothiophen-2-yl)-N-(2-(Trifluoromethyl)Phenyl)Methanimine *Sakarya University Journal of Science*, 28(5), 1070-1085. https://doi.org/10.16984/saufenbilder.1533467

also utilized in various applications, including as dyes, antioxidants, sanitizers, copolymers developers, and corrosion inhibitors [11, 12].

Molecular docking has become an essential tool in drug discovery, allowing researchers to model the interactions between a small ligand molecule and a protein at the atomic level [13]. With this method, the optimal ligand orientation that binds most effectively to a particular protein is determined and information about the intermolecular structure of the complex formed between multiple molecules is obtained [14]. The binding site's knowledge enhances docking study efficiency [15].

In this study, we have synthesized Schiff base following our previous work [16], determined their structures with single-crystal X-ray diffraction, performed computational studies with Gaussian, and carried out biological potential assessments using an in-silico docking model.

2. General Methods

2.1. Chemicals and instruments

All chemicals used for synthesis and purification were obtained from Merck. UV-Vis absorption spectrum was measured from 200 to 900 nm in ethyl alcohol using a Thermo Evolution Array UV-Vis spectrophotometer. The IR spectra of the synthesized compounds were recorded with a Perkin Elmer Spectrum Two FT-IR spectrophotometer equipped with an ATR module, covering a range of 4000-400 cm^{-1}. NMR spectra were obtained in DMSO-d_6 with a Bruker Avance III 400 MHz NMR Spectrometer.

2.2. Synthesis of (E)-1-(5-nitrothiophen-2-yl)-N-(2-(trifluoromethyl)phenyl) methanimine (N2TPM)

The title compound was synthesized following a protocol previously established by our research group [1,16]. Schiff base formed by an equimolar reaction of 5-nitro-2-thiophenecarboxaldehyde and 2-(trifluoromethyl)aniline in ethanol, with the reaction mixture refluxed for 36 hours (Figure 1). The reaction was monitored by TLC. At the end of the reaction, a burgundy product was obtained and filtered. Crystallization was carried out slowly in ethyl alcohol at room temperature.

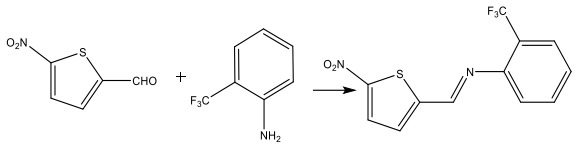

Figure 1. Synthesis scheme of N2TPM

2.3. Crystal structure analysis

Data were collected with the STOE IPDS 2 [17] diffractometer. The structure was determined using the SHELXT program [18] and the SHELXL program [19]. X-AREA was used for unit cell optimization. Molecular geometry calculations were made with WinGX [20].

2.4. Computational studies

The geometric optimization, theoretical UV-Vis spectrum, theoretical infrared spectrum, molecular orbital energies, and electronic transitions for the compound were obtained by Gaussian 09 software [21, 22]. GaussSum 3.0 was also used for visualization [23, 24]. Harmonic vibration frequencies and wavenumbers for the optimized structure were calculated using a scale factor of 0.962 [25]. Additionally, the theoretical vibrational spectrum of the synthesized compound was analyzed using Potential Energy Distribution (PED) with the assistance of the VEDA 4 program [26]. Gaussian 09, B3LYP method, and 6-31G(d,p) set were used in DFT studies [27, 28]. Results from DFT studies, including natural bond orbitals (NBO), the density of states (DOS), frontier molecular orbitals (FMO), and global reactivity parameters were analyzed using GaussView 5.0. Input files for optimization are derived from the crystal structure to ensure the best possible alignment with the data [1, 29].

2.5. Hirshfeld surfaces analysis

A Hirshfeld surface represents the outer contour of the space occupied by a molecule or an atom within a crystalline environment. In this study, Hirshfeld surfaces and 2D fingerprint plots were generated using the Crystal Explorer 17.5

program, which incorporates the TONTO software [30]. The normalized contact distance d_{norm}, based on both the external distance d_e and internal distance d_i, was calculated using a standard equation [1, 31].

2.6. In silico and In vitro assessments toward Esterases

In vitro evaluation, a spectrophotometric method was used. Docking studies of the resulting compound were carried out using the free online docking program AutoDock [1, 32]. Acetylcholinesterase (AChE) and butyrylcholinesterase (BChE) crystal structures were used for docking simulations. The results were visualized graphically using Discovery Studio Visualize.

3. Results and Discussion

3.1. Spectroscopic studies

The compound was characterized using X-ray diffraction and spectroscopic techniques. The compound depicted 257 nm and 355 nm in UV-Vis spectroscopy (Figure 2). In UV-Vis spectroscopy, the band below 290 nm was assigned to the π–π* transition, while the band above 290 nm was attributed to the n–π* transitions [33].

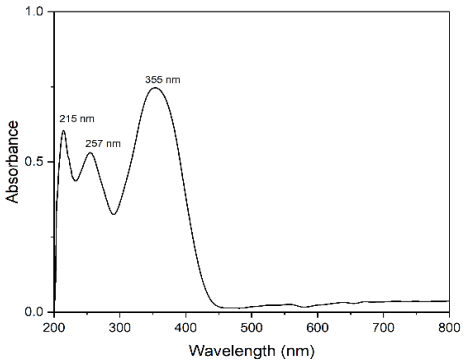

Figure 2. UV-Vis spectrum of N2TPM

Several informative bands appeared in the FT-IR spectrum in the 4000-650 cm^{-1} range. The absorption band observed between 1695-1595 cm^{-1} is characteristic of the C=N group in N2TPM [34, 35]. In FT-IR spectra of compound a strong bands appeared at 1578 cm^{-1} due to azomethine linkage. The appearance of these bands provided preliminary indications about the targeted products. Additionally, it was observed that the presence of the fluorine (F) group in the compound caused the C=N group to shift to 1578 cm^{-1}. The C=C IR band at 1535 cm^{-1} is seen in Figure 3.

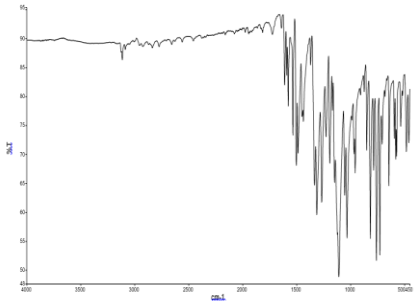

Figure 3. FT-IR spectrum of N2TPM

NMR spectra were recorded in DMSO-d_6 using a Bruker Avance III 400 MHz NMR Spectrometer. The disappearance of NH_2 and appearance of a new singlet peak in ^{1}H-NMR was assigned to HC=N at δ 8.89 which confirmed the synthesis of the targeted compound [36]. The doublet peaks at 8.20 and 7.80 correspond to protons in the thiophene ring in the compound. The signal for Ar-H was observed in the range δ 7.80-7.43 Figure 4. ^{13}C-NMR of the compound showed twelve signals from 158.14 to 14.63 ppm Fig. 5.

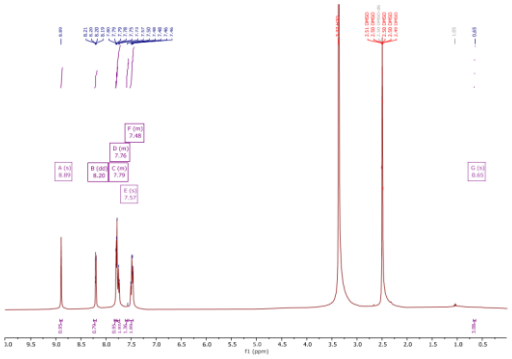

Figure 4. ^{1}H-NMR spectrum of N2TPM

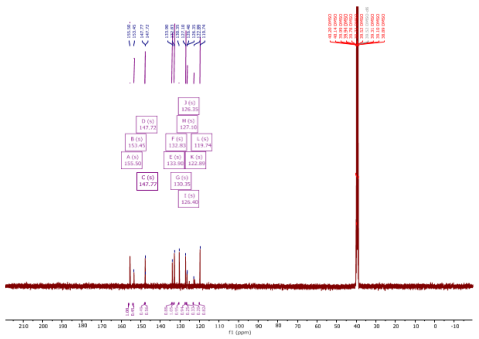

Figure 5. ^{13}C-NMR spectrum of N2TPM

Yield: 89%; m.p.: 161 °C; λ_{max}: 257 nm and 355 nm; IR: 3117 (C–H, arom.), 1578 (HC=N), 1575 (C–NO_2), 1535 (C=C), 1109 (C–O), 817 (C–S) cm^{-1}; ^{1}H-NMR (400 MHz, DMSO-d_6): δ 8.89 (s, 1H), 8.20 (dd, J = 4.0, 1.8 Hz, 1H), 7.82 – 7.77 (m, 1H), 7.80 – 7.71 (m, 2H), 7.53 – 7.43 (m, 2H); ^{13}C NMR (100 MHz, DMSO-d_6): δ 155.50 (C2), 153.45 (C6), 147.77 (C5), 147.72 (C8), 133.90 (C10), 132.83 (C4), 130.35 (C3), 127.10 (C11), 126.40 (C9), 126.35 (C12), 122.89 (C13), 119.74 (C15).

3.2. XRD Analysis

The structure of the compound was further confirmed by single-crystal X-ray analysis. Table 1 summarizes the data. Figure 6 illustrates the asymmetric unit of the compound. The compound contains two independent organic molecules and are not planar. The corresponding angles for C7–C12 and C20–C25 fluorobenzene rings are 37.22(12)˚ and 31.752(10)˚ in compound, respectively. The molecule is linked by C6—H6···O3 (−x+1, −y+1, −z+1), C19─H19···O1 (−x+1, −y+1, −z+2) and C11─H11···O4 (−x+1, −y+2, −z+1) hydrogen bonds (Figure 6 and Table 2). The C6—N1 and C19—N2 bond lengths are typical of double bonds. The N–O bond lengths [1.221(5), 1.210(5), and 1.212(5) Å] in the nitro group are close to the values observed for related compounds reported in the literature. In addition, C–F bond lengths [1.329–1.342 Å] in the trifluoromethyl group are similar to a work by Ilmi et al. [37]. Crystal packing of N2TPM is given in Figure 7.

Table 1. Crystal data and structure refinement of N2TPM

Crystal data	**Compound**
CCDC	2067648
Empirical formula	$C_{12}H_7F_3N_2O_2S$
Formula weight	300.263
Temperature/K	296
Crystal system	triclinic
Space group	P-1
a/Å	7.5965(5)
b/Å	11.0021(7)
c/Å	15.9138(10)
α/°	91.351(5)
β/°	94.741(5)
γ/°	105.750(5)
Volume/$Å^3$	1274.25(15)
Z	4
$\rho_{calc}g/cm^3$	1.565
μ/mm^{-1}	0.293
F(000)	608.9
Crystal size/mm^3	0.45 × 0.27 × 0.14
Radiation	Mo Kα (λ = 0.71073)
2Θ range for data collection/°	3.86 to 52
Index ranges	-11 ≤ h ≤ 11, -16 ≤ k ≤ 16, -24 ≤ l ≤ 22
Reflections collected	26313
Independent reflections	5021 [R_{int} = 0.1075, R_{sigma} = 0.1192]
Data/restraints/parameters	5021/0/361
Goodness-of-fit on F^2	1.003
Final R indexes [I>=2σ (I)]	R_1 = 0.0769, wR_2 = 0.1799
Final R indexes [all data]	R_1 = 0.1249, wR_2 = 0.2057
Largest diff. peak/hole / e $Å^{-3}$	0.85/-0.59

Table 2. Hydrogen-bond geometries for N2TPM (Å, °)

D—H···A	D—H	H···A	D···A	**D—H···A**
C6—H6···O3i	0.93	2.53	3.313(6)	142
C19—H19···O1ii	0.93	2.43	3.277(5)	151
C11—H11···O4iii	0.93	2.53	3.2189(6)	131

Symmetry codes: (i) −x+1, −y+1, −z+1; (ii) −x+1, −y+1,−z+2; (iii) −x+1, −y+2, −z+1. (Cg2: C6–C11 ring center)

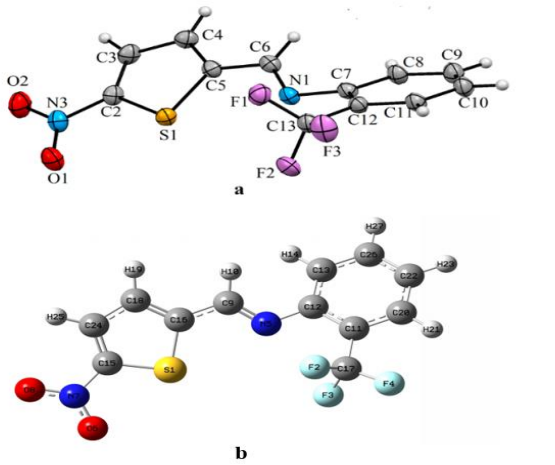

Figure 6. (**a**) Crystal unit; (**b**) Optimized structure of N2TPM (Atomic numbering used for PED analysis)

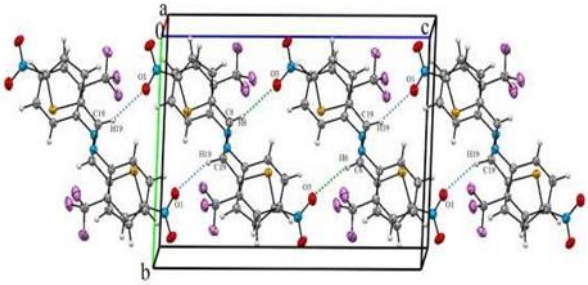

Figure 7. Crystal packing of N2TPM

3.3.Computational Studies

3.3.1. UV–Vis spectrum

Three absorption bands were observed in the experimental electronic spectrum of the compound in ethanol. The absorption observed at λ = 214 nm in the absorption spectrum corresponds to π-π∗ electronic transitions resulting from the delocalization of electrons in aromatic thiophene and benzene rings.

The absorption at λ = 256 nm, visible as the second peak detected in the experimental spectrum, is attributed to the π-π* transition in the benzene ring, thiophene, and azomethine (-HC=N-) moieties. The electronic transitions found in the calculated UV-Vis spectra between 272-339 nm are observed to occur through the benzene ring towards the thiophene ring, whereas the transitions at higher wavelengths are monitored to occur through the imine group.

The peak observed as a broad band at λ = 352 nm is the characteristic n-π∗ transition of the azomethine (C=N) group. This same transition was theoretically observed nearly at λ = 426 nm. It has been identified that the results of the experimental and theoretical studies are in good agreement with previous studies [38-42].

The calculated UV-Vis spectrum and the frontier molecular orbitals were examined utilizing Gauss-View and GaussSum and given with experimental spectrum in Figure 8. Table 3 lists the wavelengths of the experimental and calculated electronic transitions and the corresponding transitions, the energy of the transitions, the oscillator intensity, and the contribution of the orbitals to the electronic transitions.

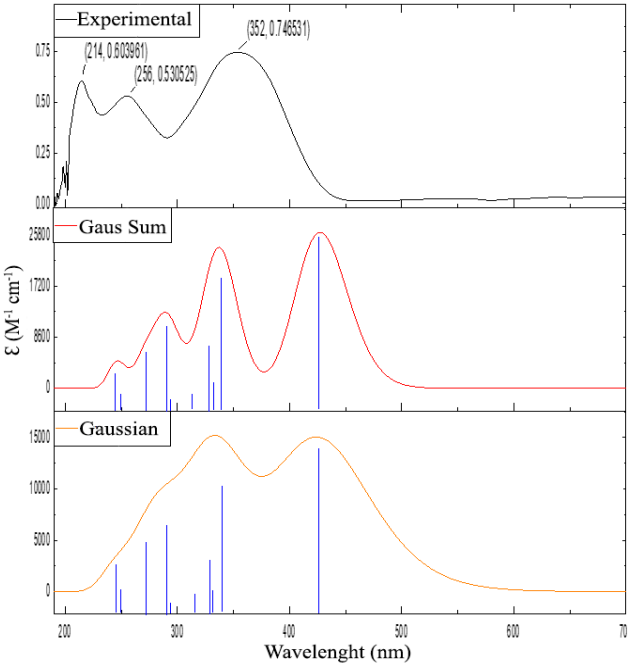

Figure 8. Experimental and calculated UV–Vis absorption spectra of N2TPM

Table 3. Assignments, energies, and wavelengths of the experimental and major theoretical transitions of N2TPM

λ exp (nm)	λ calc. (nm)	Assignment	Energy (eV)	Oscillator strengths	Major Contribution (%)
214	250.73	π-π*	4.9449	0.0159	HOMO→L+2 (45%) H-1→L+1 (33%) H-2→L+1 (14%)
	244.77	π-π*	5.0654	0.0503	H-1→L+1 (41%) H-2→L+1 (37%)
256	339.71	π-π*	3.6497	0.2446	H-1→LUMO (75%) H-4→LUMO (12%)
	331.08	π-π*	3.7449	0.0228	H-5→LUMO (65%) H-4→LUMO (11%) H-1→LUMO (13%)
	328.91	π-π*	3.7696	0.0718	H-2→LUMO (91%)
	314.91	π-π*	3.9371	0.0184	H-3→LUMO (95%)
	293.57	π-π*	4.2233	0.0048	H-6→LUMO (88%)
	290.63	π-π*	4.2660	0.1517	HOMO→L+1 (53%) H-4→LUMO (25%)
	272.04	π-π*	4.5576	0.0843	H-4→LUMO (45%) H-5→LUMO (10%) HOMO→L+1 (37%)
352	426.84	n-π*	2.9047	0.3621	HOMO→LUMO (94%)

3.3.2. Vibration spectral analysis

The experimental and theoretical FT-IR spectra of the compound are presented in Figure 9. In Table 4 the experimental and calculated values of the wave numbers of the vibrations in the molecule are provided along with the % PED values. The experimental aromatic C-H stretching vibrations of the thiophene and benzene rings in the structure of the compound were observed in the range of 3126 to 3046 cm^{-1} [43]. The theoretical wavelengths corresponding to these vibrations were calculated as 3140, 3110, 3102, 3090, 3082, and 3068 cm^{-1}, respectively.

The C-H stretching vibration of the imine group was found experimentally at 2927 cm^{-1} and was found to be in good agreement with the theoretical value of 2928 cm^{-1}. In previous studies, it has been reported that the stretching frequencies for C=C bonds in the aromatic ring are typically observed between 1625 and 1430 cm^{-1} [44, 45]. The experimental vibrations for C=C bonds were recorded at 1592, 1578, and 1488 cm^{-1}, while the theoretical vibrations were recorded at 1585, 1568, and 1472 cm^{-1}, respectively. Furthermore, the vibrational frequency of the C=C bond in the thiophene ring was determined experimentally at 1503 cm^{-1} and found computationally at 1523 cm^{-1}.

The calculated value for the azomethine ν(C=N) vibration of the N2TPM is 1627 cm^{-1}, while the observed experimental value is 1592 cm^{-1}. The experimental observation determined the asymmetric vibration of the N-O bond at a frequency of 1535 cm^{-1}, which is different from the calculated value of 1564 cm^{-1}. Similarly, the symmetric stretching of ν(N-O) was experimentally detected at 1334 cm^{-1} and is almost identical to the calculated value of 1335 cm^{-1}.

The symmetric vibration of the ν(SC) bond was detected experimentally at 1149 cm^{-1} and theoretically at 1153 cm^{-1}. The bending vibrations of the C-S bond were found at 708 cm^{-1} in the experimental spectrum and 713 cm^{-1} in the calculation method.

The stretching vibrations of the symmetric and antisymmetric CF_3 groups typically occur between 1290-1235 cm^{-1} and 1226-1200 cm^{-1}, respectively [46]. For this compound, these stretching vibrations were observed experimentally between 1268-1149 cm^{-1} and theoretically between 1285-1153 cm^{-1}.

The correlation plots in Figure 10 obtained using the experimental and theoretical wavenumbers were analyzed and it was found that plot B had a

stronger R^2 value than plot A, indicating a better agreement of the experimental data with the scaled theoretical frequencies.

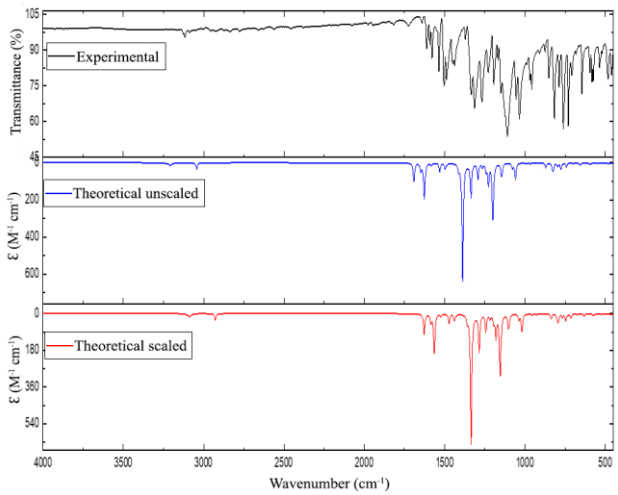

Figure 9. Comparative illustration of experimental and theoretical spectrum of N2TPM

3.3.3. Molecular orbitals

The bond lengths and angles of the resulting compound were analyzed by comparing them with theoretical density functional theory results and experimental X-ray diffraction data. The comparison showed a close agreement between the experimental and theoretical studies, as detailed in Tables 5, and 6. The R^2 values were 0.9914 for bond lengths and 0.9859 for bond angles, as shown in Figures 11 and 12. These high R^2 values indicate a strong agreement between the experimental and theoretical structural parameters, with values close to 1.0.

Small differences in bond angles may be attributed to the distinction between gaseous phase calculations in DFT and solid phase measurements in XRD studies. DFT calculations were also used to determine the compound's

Table 4. Experimental and theoretical wavenumbers and PED analysis of N2TPM.

Experimental (cm^{-1})	Calculated (unscaled) (cm^{-1})	Calculated (scaled with 0.962) (cm^{-1})	Vibration source	Assignment (PED%) Atom number
3126	3264	3140	Tiophene moiety	ν CH (97) → $C_{24}H_{25}$
3117	3234	3110	Benzene moiety	ν CH (91) → $C_{20}H_{21}$
3076	3213	3090	Benzene moiety	ν CH (91) → $C_{13}H_{14}$ + $C_{22}H_{23}$ + $C_{26}H_{27}$
3061	3204	3082	Benzene moiety	ν CH (95) → $C_{13}H_{14}$ + $C_{22}H_{23}$
3046	3190	3068	Benzene moiety	ν CH (97) → $C_{13}H_{14}$ + $C_{22}H_{23}$ + $C_{26}H_{27}$
2927	3044	2928	Imine moiety	ν CH (100) → C_9H_{10}
1612	1691	1627	Imine moiety	ν NC (69) → N_5C_9
1592	1649	1585	Benzene moiety	ν CC (59) → $C_{11}C_{20}$ + $C_{13}C_{26}$ + $C_{20}C_{22}$ + $C_{12}C_{13}$
1578	1630	1568	Benzene moiety	ν CC (41) → $C_{22}C_{26}$
1535	1626	1564	NO_2 moiety	ν NO (89) → N_7O_6+ N_7O_8
1503	1584	1523	Tiophene moiety	ν CC (58) → $C_{15}C_{24}$ + $C_{16}C_{18}$
1488	1531	1472	Benzene moiety	β CCC (23) → $C_{12}C_{13}C_{26}$ +$C_{13}C_{26}C_{22}$ + $C_{20}C_{22}C_{26}$ β HCC (15) → $H_{21}C_{20}C_{22}$ β HCC (25) → $H_{14}C_{13}C_{26}$ + $H_{23}C_{22}C_{26}$
1334	1388	1335	NO_2 moiety	ν NO (75) → N_7O_6 + N_7O_8

Table 4. Experimental and theoretical wavenumbers and PED analysis of N2TPM (Continue)

Experimental (cm^{-1})	Calculated (unscaled) (cm^{-1})	Calculated (scaled with 0.962) (cm^{-1})	Vibration source	Assignment (PED%) Atom number
1228	1293	1243	CF_3 moiety	ν FC(11) → F_2C_{17} + F_3C_{17}
1168	1202	1156	CF_3 moiety	ν FC (60) → F_3C_{17} + F_4C_{17}
1149	1199	1153	CF_3 moiety	ν FC (61) → F_2C_{17} + F_3C_{17}
1109	1148	1104	Tiophene moiety	ν SC (60) → S_1C_{15}
817	823	792	NO_2 moiety	β ONO(58) → $O_8N_7O_6$
729	742	713	NO_2 moiety	γ OCON(85) → $O_8C_{15}O_6N_7$
708	689	674	Tiophene moiety	β SCC (41) → $S_1C_{15}C_{24}$

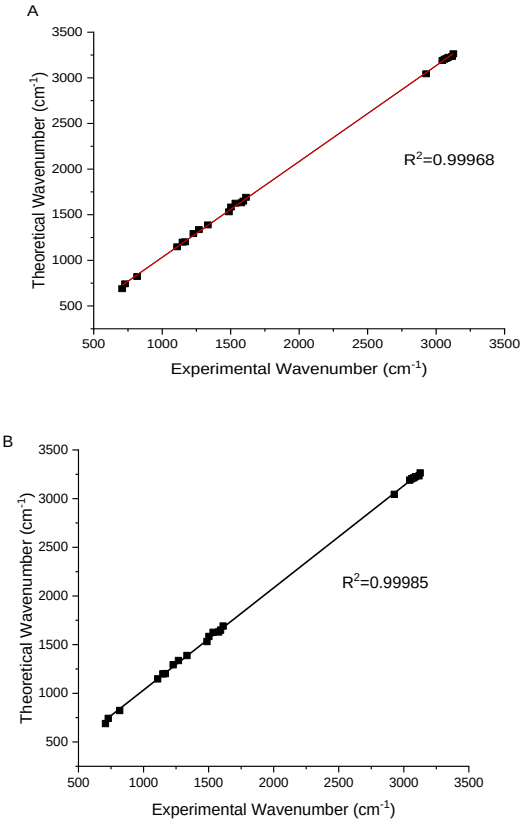

Figure 10. Correlation graphs of (A) experimental wavenumber-theoretical wavenumber (not scaled), (B) experimental wavenumber-theoretical wavenumber (scaled with 0.962)

HOMO and LUMO orbitals as well as different inter-orbital energy gaps. An energy difference of 4.724 eV was found between HOMO and LUMO, and an energy difference of 7.676 eV was found between HOMO-1 and LUMO+1 (Figure 13). This energy difference between HOMO and LUMO suggests that the molecule is relatively stabilized [47].

Table 5. Bond lengths of N2TPM

Atom	Atom	Length/Å	
		XRD	DFT
S1	C2	1.710(4)	1.72936
S1	C5	1.716(4)	1.73687
F1	C13	1.333(6)	1.35189
F2	C13	1.342(6)	1.35187
F3	C13	1.336(5)	1.34760
N1	C6	1.271(5)	1.27440
N1	C7	1.413(6)	1.39868
O1	N3	1.221(5)	1.22695
N3	O2	1.221(5)	1.22909
N3	C2	1.430(6)	1.43827
C12	C7	1.402(6)	1.40857
C12	C13	1.483(6)	1.50831
C12	C11	1.385(6)	1.38926
C6	C5	1.447(6)	1.44633
C2	C3	1.354(6)	1.36932
C7	C8	1.416(6)	1.39972
C8	C9	1.352(7)	1.38845
C5	C4	1.371(6)	1.38083
C4	C3	1.400(7)	1.40720
C10	C11	1.372(6)	1.39097
C10	C9	1.383(7)	1.38884

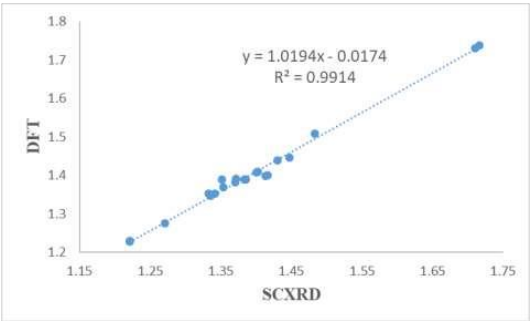

Figure 11. Correlation of bond length between DFT and SCXRD of N2TPM

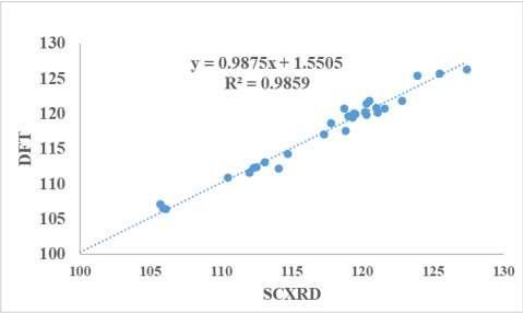

Figure 12. Correlation of bond angle between DFT and SCXRD of N2TPM

Table 6. Bond angles of N2TPM

Atom	Atom	Atom	Length/Å	
			XRD	DFT
C5	S1	C2	89.4(2)	89.38666
C6	C5	S1	120.3(3)	121.42081
C10	C9	C8	121.1(4)	120.15856
C7	N1	C6	118.7(4)	120.70378
O2	N3	O1	123.9(5)	125.39812
C2	N3	O1	117.3(4)	117.07657
C2	N3	O2	118.8(4)	117.52528
F3	C13	F2	105.7(4)	107.09661
C12	C13	F1	114.1(4)	112.24987
C12	C13	F2	112.5(4)	112.41674
C12	C13	F3	112.0(4)	111.63392
C13	C12	C7	120.2(4)	120.20031
C11	C12	C7	119.5(4)	119.95297
C11	C12	C13	120.3(4)	119.84233
C5	C6	N1	120.5(4)	121.86881
C4	C5	S1	112.3(4)	112.31070
C4	C5	C6	127.4(4)	126.26849
F2	C13	F1	105.9(4)	106.57544
F3	C13	F1	106.1(4)	106.47915
C3	C2	S1	114.7(4)	114.28557
C3	C2	N3	125.9(4)	125.71288
N3	C2	S1	119.4(3)	120.00154
C3	C4	C5	113.1(4)	113.06748
C9	C10	C11	119.0(5)	119.63679
C4	C3	C2	110.5(4)	110.94952
C10	C11	C12	121.6(4)	120.72574
C12	C7	N1	119.3(4)	119.41970
C8	C7	N1	122.8(4)	121.81181
C8	C7	C12	117.8(4)	118.67699
C9	C8	C7	121.0(4)	120.82674

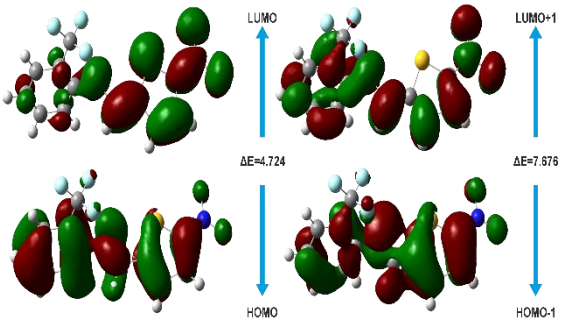

Figure 13. HOMO and LUMO of N2TPM

3.3.4. Natural bond orbitals

Gaussian software was used to calculate the Natural Bond Orbitals of the resulting compound. NBO analysis provides information about individual bonds in the molecule and the associated energies of lone pair and bond pair electrons, which helps understand atomic interactions. This analysis allows for the prediction of the behavior of donor and acceptor atoms within the molecule.

The NBO data for the compound, as listed in Table 7, show that the highest energy interaction is between C12-C13 and C11-C12, with an energy of 4.48 kcal/mol. The lowest energy interaction is between S1-C16 and C18, with an energy of 2.12 kcal/mol, where F2 acts as the donor and C17 as the acceptor.

Table 7. NBO of the N2TPM

Donor (i)	Acceptor (j)	E(2) [Kcal/ mol]	E(j)E(i) (a.u)	F(I.J) (a.u)
S1-C15	C16	0.59	1.70	0.028
S1-C16	C18	0.53	1.37	0.024
N5-C9	C11-C12	1.95	1.47	0.048
O6-N7	C15	1.92	2.00	0.056
N7-C15	O6	1.57	1.97	0.050
C9-H10	N5	0.56	1.60	0.027
C11-C17	C20	1.36	1.77	0.044
C12-C13	C11-C12	4.48	1.27	0.070
F2	C17	2.12	25.08	0.207
O8	N7	0.97	15.21	0.199

3.3.5. Density of state

The density of states (DOS) for the synthesized compound was computed from the optimized and calculated using GaussSum software. This analysis is crucial for determining the various energy states or levels within the molecule, which is essential for understanding electron excitation from the ground state.

As depicted in Figure 14, the DOS spectra reveal that the energy difference between HOMO-1 and LUMO+1 varies between compounds. The net energy difference among the frontier molecular orbitals (FMOs) is 2.952 eV.

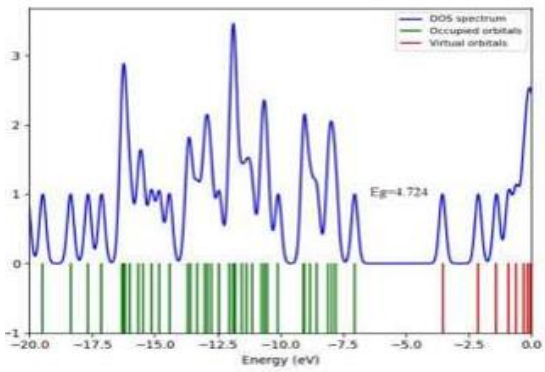

Figure 14. DOS spectra of the N2TPM

3.3.6. Global reactivity parameters

The compound shows high electronegativity due to fluorine atoms. The compound's electron affinity and ionization potential are 4.777 eV and 9.499 eV, respectively (Table 8). The chemical potential and chemical hardness values indicate favorable kinetic stability for the compound.

Table 8. Global reactivity parameters of the N2TPM

x	μ	ŋ	IP	EA	1/2ŋ	ω
7.138	-7.138	2.362	9.499	4.777	0.211	10.786

3.4.Hirshfeld Surface Analysis

Hirshfeld surface analysis (HS) is primarily used to study intermolecular interactions in crystalline compounds that contribute to crystal stabilization. The parameters d_e (distance to the nearest outer nucleus) and d_i (distance to the nearest inner nucleus) are taken into account with respect to the van der Waals radius. HS is visualized with red, blue, and white colors representing different distances relative to the total radius [16, 48].

Hirshfeld surfaces for the compound were generated with high surface resolution, mapped over the ranges −0.55 to 1.0 Å for d_{norm}, shape index from −0.10 to 1.0 Å, and curvature over the ranges −0.40 to 4.0 Å. The surfaces were made transparent to show the molecular environment around them clearly.

To identify close contacts, the d_{norm} surface was analyzed with values ranging from negative to positive. Negative values represent shorter contacts compared to van der Waals radii, while positive values represent longer contacts. Red areas on the surface indicate closer contacts at negative $d$norm values, blue areas indicate longer contacts at positive d_{norm} values, and white areas indicate distances at zero (Figure 15)

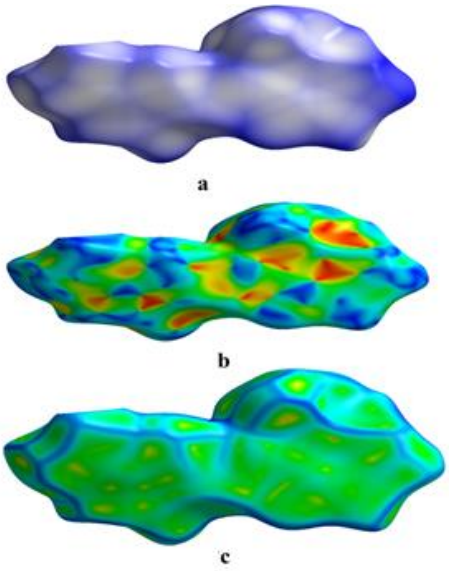

Figure 15. Hirshfeld surfaces are mapped at three views; (a) dnorm, (b) shape index, and (c) curvature.

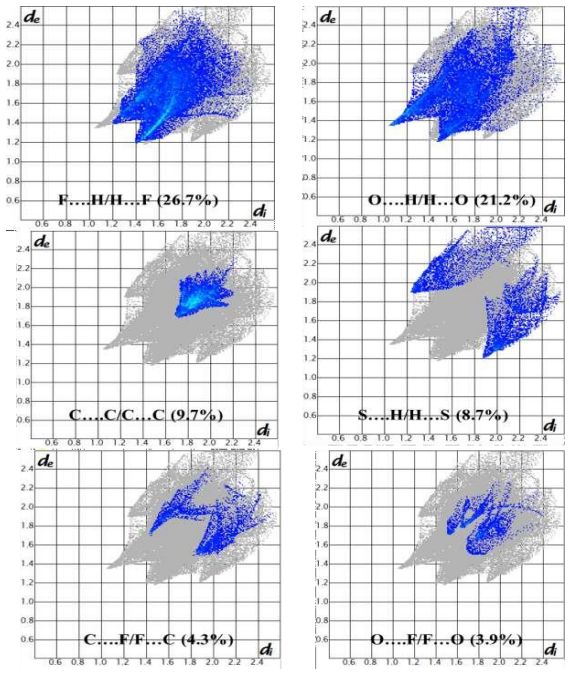

Figure 16. Fingerprint plots of contacts along with relative contributions for N2TPM

2 D fingerprint plots of under studied compound were mapped to check the connections between atoms as shown in Figure 16. It was observed from contacts that H….F/F….H (26.7%). Interactions are major contributors to compound. O...H/H…O (21.2%) are the second major contributing contacts in compound. The

compound has depicted contacts C…C (9.7%), S…H/H…S (8.7%), C…F/F…C (4.3%), and O…F/F…O (3.9%).

3.5. In silico and in vitro enzyme inhibition

The esterase family, which includes enzymes such as acetylcholinesterase (AChE) and butyrylcholinesterase (BChE), plays an important role in Alzheimer's disease. Table 9 details the in vitro potential of the synthesized compound. Docking studies using energy-based scoring functions help determine the optimal conformation of a ligand when binding to a target protein [15]. In general, lower energy scores indicate better binding affinity between protein and ligand [49], making it very important to identify ligand binding modes with the lowest energy values [50].

The results indicate that the compound can act as an enzyme inhibitor, exhibiting significant docking scores and binding energies (Table 9). Specifically, the compound showed a docking score of -10.4159, a binding energy of -10.2743 with AChE, a docking score of -10.3378, and a binding energy of -9.8889 with BChE.

The phenyl ring of the compound displayed π-π interactions with Trp279 and Trp334, while the thiophene moiety showed similar interactions with Phe330. The fluorine atom within the molecule formed strong hydrogen bonds with Phe288 on AChE. Additionally, the residues Phe331 and His440, located at the active sites, interacted with the compound, helping to anchor it at the active site of AChE (Figure 17).

Similarly, the compound showed firm binding with various amino acid residues at the active site of BChE, including Trp82, Glu443, and Gly155, through strong hydrogen bonding interactions involving the fluorine atom and the nitro group's oxygen. The compound also exhibited π-alkyl and π-π interactions between the five-membered ring of the N2TPM and the phenyl ring of Trp82, along with Ala328 and Leu450 (Figure 18).

Table 9. Docking Results of the N2TPM

Docking Score (Kcal/mol)		Enzyme Inhibition (%age)	
AChE	**BChE**	**AChE**	**BChE**
-10.4159	-10.3378	66.42 ± 1.1	65.20± 1.0

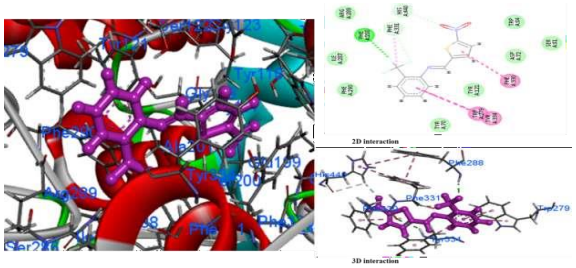

Figure17. 3D Interactions of N2TPM on active sites of AChE

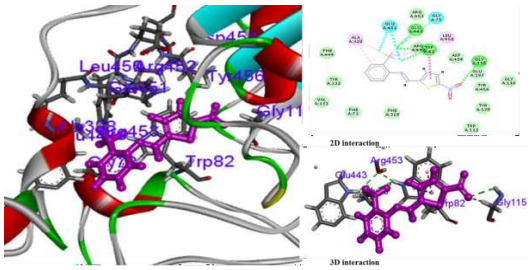

Figure 18. 3D Interactions of N2TPM on active sites of BChE

4. Conclusion

In organic chemistry, new bioactive molecules are constantly being developed for human health. Schiff bases show significant potential and active effects in the treatment of many diseases. In this study, a Schiff base containing heterocyclic components was synthesized and its structure was elucidated by spectroscopic techniques. The crystal structure of the compound was analyzed using 2D and 3D plots, which showed the crystal stability due to various interactions through Hirshfeld surface analysis.

The crystal structure was optimized using Gaussian software and the results were compared with X-ray diffraction (XRD) data, which showed a close agreement in bond angles and lengths. Gaussian calculations have shown that the molecule has remarkable kinetic stability, providing information on various structural parameters such as chemical potential, chemical hardness, electronegativity, and electron affinity.

The biological activity of the synthesized Schiff base was assessed through enzyme inhibition assays targeting acetylcholinesterase (AChE) and butyrylcholinesterase (BChE), enzymes linked to neurodegenerative disorders such as Alzheimer's disease. Both in vitro and in silico studies demonstrated strong inhibitory activity against AChE and BChE, suggesting that the compound possesses significant potential as a

therapeutic agent. Molecular docking studies further supported these findings, revealing favorable binding interactions within the active sites of the target enzymes.

Article Information Form

Acknowledgments
The author would like to thank Dr. Taşkın Basılı for his contributions.

Funding
The author has not received any financial support for this study's research, authorship or publication.

The Declaration of Conflict of Interest/ Common Interest
No conflict of interest or common interest has been declared by the authors.

The Declaration of Ethics Committee Approval
This study does not require ethics committee permission or any special permission.

The Declaration of Research and Publication Ethics
The authors of the paper declare that they comply with the scientific, ethical and quotation rules of SAUJS in all processes of the paper and that they do not make any falsification on the data collected. In addition, they declare that Sakarya University Journal of Science and its editorial board have no responsibility for any ethical violations that may be encountered, and that this study has not been evaluated in any academic publication environment other than Sakarya University Journal of Science.

References

[1] M. A. Raza, N. Dege, O. E. Dogan, T. Agar, S. H. Sumrra, "Synthesis of two new Schiff bases; crystal structure, Hirshfeld surface analysis, density functional theory and molecular docking," Journal of Molecular Structure, vol. 1226, p. 129330, 02/15/ 2021.

[2] R. Kataria, D. Vashisht, P. Rani, J. Sindhu, S. Kumar, S. Sharma, S. C. Sahoo, V. Kumar, S. Kumar Mehta, "Experimental and Computational Validation of Structural Features and BSA Binding Tendency of 5-Hydroxy5trifluoromethyl3arylpyrazolines, " Chemistry Select, vol. 6, no. 38, pp. 10324-10335, 2021.

[3] N. Dege, M. A. Raza, O. E. Doğan, T. Ağar, M. W. Mumtaz, "Theoretical and experimental approaches of new Schiff bases: efficient synthesis, X-ray structures, DFT, molecular modeling and ADMET studies," Journal of the Iranian Chemical Society, vol. 18, no. 9, pp. 2345-2368, 09/01/ 2021.

[4] M. Shakir, N. Shahid, N. Sami, M. Azam, A. U. Khan, "Synthesis, spectroscopic characterization and comparative DNA binding studies of Schiff base complexes derived from L-leucine and glyoxal," (in eng), Spectrochim Acta A Mol Biomol Spectrosc, vol. 82, no. 1, pp. 31-36, 2011.

[5] S. Zolezzi, E. Spodine, A. Decinti, "Electrochemical studies of copper(II) complexes with Schiff-base ligands," Polyhedron, vol. 21, no. 1, pp. 55-59, 01/15/ 2002.

[6] P. G. Cozzi, "Metal–Salen Schiff base complexes in catalysis: practical aspects," Chemical Society Reviews, vol. 33, no. 7, pp. 410-421, 2004.

[7] H. Zafar, A. Ahmad, A. U. Khan, T. A. Khan, "Synthesis, characterization and antimicrobial studies of Schiff base complexes," Journal of Molecular Structure, vol. 1097, pp. 129-135, 10/05/ 2015.

[8] P. Arora, V. Arora, H. Lamba, D. Wadhwa, "Importance of heterocyclic chemistry: A review," International Journal of

Pharmaceutical Sciences and Research, vol. 3, no. 9, p. 2947, 2012.

[9] T. Kunied, H. Mutsanga, "The chemistry of heterocyclic compounds," Palmer (B), vol. 175, 2002.

[10] M. S. Saini, A. Kumar, J. Dwivedi, R. Singh, "A review: biological significances of heterocyclic compounds," International Journal of Pharma Sciences and Research, vol. 4, no. 3, pp. 66-77, 2013.

[11] J. Zhang, W. Liu, Q. Xue, "The effect of molecular structure of heterocyclic compounds containing N, O and S on their tribological performance," Wear, vol. 231, no. 1, pp. 65-70, 1999.

[12] A. W. Czarnik, "Guest Editorial," Accounts of Chemical Research, vol. 29, no. 3, pp. 112-113, 03/13/1996.

[13] B. J. McConkey, V. Sobolev, M. Edelman, "The performance of current methods in ligand-protein docking," Current Science, vol. 83, pp. 845-856, 2002.

[14] N. K. Sharma, K. Jha, "Molecular docking: an overview," Journal of Advanced Scientific Research, vol. 1, no. 1, pp. 67-72, 2010.

[15] A. Vijesh, A. M. Isloor, S. Telkar, T. Arulmoli, H.-K. Fun, "Molecular docking studies of some new imidazole derivatives for antimicrobial properties," Arabian Journal of Chemistry, vol. 6, no. 2, pp. 197-204, 2013.

[16] Raza, M. A., Farwa, U., Danish, M., Ozturk, S., Aagar, A. A., Dege, N., Rehman, S. U., Al-Sehemi, A. G., "Computational modeling of imines based anti-oxidant and anti-esterases compounds: Synthesis, single crystal and In-vitro assessment," Computational Biology and Chemistry, vol. 104, p. 107880, 06/01/ 2023.

[17] C. Stoe, "X-area (version 1.18) and X-red32 (version 1.04)," Stoe & Cie, Darmstadt, *Germany*, 2002.

[18] G. M. Sheldrick, "SHELXT–Integrated space-group and crystal-structure determination," Acta Crystallographica Section A: Foundations and Advances, vol. 71, no. 1, pp. 3-8, 2015.

[19] G. M. Sheldrick, "Crystal structure refinement with SHELXL," Acta Crystallographica Section C: Structural Chemistry, vol. 71, no. 1, pp. 3-8, 2015.

[20] L. J. Farrugia, "WinGX suite for small-molecule single-crystal crystallography," journal of Applied Crystallography, vol. 32, no. 4, pp. 837-838, 1999.

[21] A. D. Becke, "Density-functional exchange-energy approximation with correct asymptotic behavior," Physical review A, vol. 38, no. 6, p. 3098, 1988.

[22] C. Lee, W. Yang, R. G. Parr, "Development of the Colle-Salvetti correlation-energy formula into a functional of the electron density," Physical review B, vol. 37, no. 2, p. 785, 1988.

[23] R. Dennington, T. Keith, J. Millam, "GaussView, Version 4.1. 2," Semichem Inc., *Shawnee Mission, KS*, 2007.

[24] N. M. O'boyle, A. L. Tenderholt, K. M. Langner, "Cclib: a library for package-independent computational chemistry algorithms," Journal of computational chemistry, vol. 29, no. 5, pp. 839-845, 2008.

[25] M. P. Andersson, P. Uvdal, "New scale factors for harmonic vibrational frequencies using the B3LYP density functional method with the triple-ζ basis set 6-311+ G (d, p)," The Journal of Physical Chemistry A, vol. 109, no. 12, pp. 2937-2941, 2005.

[26] M. H. Jamróz, "Vibrational energy distribution analysis (VEDA): scopes and limitations," Spectrochimica Acta Part A: Molecular and Biomolecular Spectroscopy, vol. 114, pp. 220-230, 2013.

[27] A. D. Becke, "Density-functional thermochemistry. I. The effect of the exchange-only gradient correction," The Journal of chemical physics, vol. 96, no. 3, pp. 2155-2160, 1992.

[28] M. J. Frisch, G. W. Trucks, H. B. Schlegel, G. E. Scuseria, M. A. Robb, J. R. Cheeseman, G. Scalmani, V. Barone, B. Mennucci, G. A. Petersson, H. Nakatsuji, M. Caricato, X. Li, H. P. Hratchian, A. F. Izmaylov, J. Bloino, G. Zheng, J. L. Sonnenberg, M. Hada, M. Ehara, K. Toyota, R. Fukuda, J. Hasegawa, M. Ishida, T. Nakajima, Y. Honda, O. Kitao, H. Nakai, T. Vreven, J. A. Montgomery, Jr., J. E. Peralta, F. Ogliaro, M. Bearpark, J. J. Heyd, E. Brothers, K. N. Kudin, V. N. Staroverov, R. Kobayashi, J. Normand, K. Raghavachari, A. Rendell, J. C. Burant, S. S. Iyengar, J. Tomasi, M. Cossi, N. Rega, J. M. Millam, M. Klene, J. E. Knox, J. B. Cross, V. Bakken, C. Adamo, J. Jaramillo, R. Gomperts, R. E. Stratmann, O. Yazyev, A. J. Austin, R. Cammi, C. Pomelli, J. W. Ochterski, R. L. Martin, K. Morokuma, V. G. Zakrzewski, G. A. Voth, P. Salvador, J. J. Dannenberg, S. Dapprich, A. D. Daniels, Ö. Farkas, J. B. Foresman, J. V. Ortiz, J. Cioslowski, D. J. Fox, *Gaussian 09* (Gaussian, Inc., Wallingford CT, 2009)., vol. 121, pp. 150-166, 2009.

[29] M. Danish, A. Bibi, K. Gilani, M. Asam Raza, M. Ashfaq, M. Nadeem Arshad, A. M. Asiri, K. Ayub, "Antiradical, antimicrobial and enzyme inhibition evaluation of sulfonamide derived esters; synthesis, X-Ray analysis and DFT studies," Journal of Molecular Structure, vol. 1175, pp. 379-388, 2019.

[30] S. Wolff, D. Grimwood, J. McKinnon, M. Turner, D. Jayatilaka, M. Spackman, "Crystal explorer," ed: University of Western Australia Perth, 2012.

[31] K. Azouzi, B. Hamdi, R. Zouari, A. b. Salah, "Synthesis, structure and Hirshfeld surface analysis, vibrational and DFT investigation of (4-pyridine carboxylic acid) tetrachlorocuprate (II) monohydrate," Bulletin of Materials Science, vol. 40, pp. 289-299, 2017.

[32] M. A. Raza, K. Fatima, Z. Saqib, J. K. Maurin, A. Budzianowski, "Designing of diamino based esterases inhibitors; synthesis, characterization, density functional theory and molecular modeling," Journal of Molecular Structure, vol. 1195, pp. 712-722, 2019.

[33] Z. H. Chohan, M. Hanif, "Design, synthesis, and biological properties of triazole derived compounds and their transition metal complexes," Journal of Enzyme Inhibition and Medicinal Chemistry, vol. 25, no. 5, pp. 737-749, 10/01/2010.

[34] É. Tozzo, S. Romera, M. P. dos Santos, M. Muraro, R. H. de A. Santos, L.M. Lião, L. Vizotto, E. R. Dockal, "Synthesis, spectral studies and X-ray crystal structure of N,N′-(±)-trans-1,2-cyclohexylenebis(3-ethoxysalicylideneamine) H2(t-3-EtOsalchxn)," Journal of Molecular Structure, vol. 876, no. 1, pp. 110-120, 03/30/2008.

[35] A. Bartyzel, "Synthesis, thermal study and some properties of N2O4—donor Schiff base and its Mn(III), Co(II), Ni(II), Cu(II) and Zn(II) complexes," Journal of Thermal Analysis and Calorimetry, vol. 127, pp. 2133-2147, 2017.

[36] A. U. Hassan, S. H. Sumrra, M. A. Raza, M. Zubair, M. N. Zafar, E. U. Mughal, M. F. Nazar, A. Irfan, M. Imran, M.A. Assiri, "Design, facile synthesis, spectroscopic characterization, and medicinal probing of metal-based new sulfonamide drugs: A theoretical and spectral study," Applied Organometallic Chemistry, vol. 35, no. 1, p. e6054, 2021.

[37] R. Ilmi, S. Kansız, N. K. Al-Rasbi, N. Dege, P. R. Raithby, M. S. Khan, "Towards white light emission from a hybrid thin film of a self-assembled ternary samarium (III) complex," New Journal of Chemistry, vol. 44, no. 15, pp. 5673-5683, 2020.

[38] A. Bashir, I. Siraj, "Synthesis, Characterization and Antimicrobial Studies of Schiff Base Derived from the Reaction of 2-Thiophenecarboxaldehyde and Ethylenediamine and its Metal (II) Complexes," ChemSearch Journal, vol. 12, no. 1, pp. 143-148, 2021.

[39] E. Ermiş, K. Durmuş, "Novel thiophene-benzothiazole derivative azomethine and amine compounds: Microwave assisted synthesis, spectroscopic characterization, solvent effects on UV–Vis absorption and DFT studies," Journal of Molecular Structure, vol. 1217, p. 128354, 2020.

[40] M. I. Jaafar, R. K. Ahmed, A.J. M. Al-Karawi, Al. Bariz OmarAli, S.Kansız, Y. Sert, N. Dege, "Synthesis, structural studies, Hirshfeld surface analysis, and molecular docking studies of a thiophene-based Schiff base compound," Journal of Molecular Structure, vol. 1265, p. 133477, 2022.

[41] M. Shakir, A. Abbasi, M. Azam, A. U. Khan, "Synthesis, spectroscopic studies and crystal structure of the Schiff base ligand L derived from condensation of 2-thiophenecarboxaldehyde and 3, 3′-diaminobenzidine and its complexes with Co (II), Ni (II), Cu (II), Cd (II) and Hg (II): Comparative DNA binding studies of L and its Co (II), Ni (II) and Cu (II) complexes," Spectrochimica Acta Part A: Molecular and Biomolecular Spectroscopy, vol. 79, no. 5, pp. 1866-1875, 2011.

[42] M. N. Uddin, D. A. Chowdhury, M. M. Rony, M. E. Halim, "Metal complexes of Schiff bases derived from 2-thiophenecarboxaldehyde and mono/diamine as the antibacterial agents," Modern Chemistry, vol. 2, no. 2, pp. 6-14, 2014.

[43] C. N. R. Rao, "Chemical applications of infrared spectroscopy," in Chemical applications of infrared spectroscopy, 1963, pp. 681-681.

[44] S.-J. Koyambo-Konzapa, R. Premkumar, R. V. Berthelot Saïd Duvalier, M. K. Gilbert Yvon, M. Nsangou, A. M. F. Benial, "Electronic, spectroscopic, molecular docking and molecular dynamics studies of neutral and zwitterionic forms of 3, 4-dihydroxy-l-phenylalanine: A novel lung cancer drug," Journal of Molecular Structure, vol. 1260, p. 132844, 07/15/2022.

[45] V. K. Rastogi, M. A. Palafox, R. P. Tanwar, L. Mittal, "3,5-Difluorobenzonitrile: ab initio calculations, FTIR and Raman spectra," Spectrochimica Acta Part A: Molecular and Biomolecular Spectroscopy, vol. 58, no. 9, pp. 1987-2004, 07/01/2002.

[46] D. G. Iraiyadian, S. J. Vedhagiri, M. Govindarajan, K. Parimala, "Molecular Dynamic Simulation Studies of 4-(Trifluoromethyl) phenylacetonitrile," Bulgarian Journal of Physics, vol. 48, no. 4, 2021.

[47] D. Li Ping, F. H. Zhang, Y. S. Zhu, C. Lu, X. Yu Kuang, J. LvPeng Shao, "Understanding the structural transformation, stability of medium-sized neutral and charged silicon clusters," (in eng), *Scientific Reports*, vol. 5, p. 15951, Nov 3 2015.

[48] T. Hökelek, S. Özkaya, H. Necefoğlu, "Crystal structure and Hirshfeld surface analysis of aqua-bis-(nicotinamide-κN(1))bis-(2,4,6-tri-methyl-benzoato-κ(2)O,O')cadmium(II)," (in eng), Acta Crystallogr E Crystallogr Commun, vol. 74, no. Pt 2, pp. 246-251, Feb 1 2018.

[49] R. Thomsen, M. H. Christensen, "MolDock: A New Technique for High-

Accuracy Molecular Docking," Journal of Medicinal Chemistry, vol. 49, no. 11, pp. 3315-3321, 06/01/2006.

[50] D. S. Goodsell, A. J. Olson, "Automated docking of substrates to proteins by simulated annealing," (in eng), Proteins, vol. 8, no. 3, pp. 195-202, 1990.